Particuology 23 (2015) 49–55

Contents lists available at ScienceDirect

Particuology

journal homepage: www.elsevier.com/locate/partic

Rolling and sliding in 3-D discrete element models

Yucang Wang[a,*], Fernando Alonso-Marroquin[b], William W. Guo[a]

[a] School of Engineering and Technology, Central Queensland University, Australia
[b] School of Civil Engineering, The University of Sydney, Australia

ARTICLE INFO

Article history:
Received 25 August 2014
Received in revised form
15 December 2014
Accepted 2 January 2015
Available online 9 May 2015

Keywords:
Discrete element method
Rolling
Sliding

ABSTRACT

Rolling and sliding play fundamental roles in the deformation of granular materials. In simulations of granular flow using the discrete element method (DEM), the effect of rolling resistance at contacts should be taken into account. However, even for the simplest case involving spherical particles, there is no agreement on what is the best way to define rolling and sliding; various versions of definitions and calculations of rolling and sliding were proposed. Some even suggest that a unique definition for rolling and sliding is not possible. We re-check previous studies on rolling and sliding in DEMs and find that some researchers made a conceptual mistake when dealing with pure sliding between particles of different sizes. After considering the particle radius in the derivation of rolling velocity, the results yield a unique solution. Starting with clear and unique definitions of pure rolling and sliding, we present the detailed derivation and validate our results by checking two special cases of rolling. The decomposition of the relative motion is *objective*; that is, independent of the reference frame in which the relative motion is measured.

Introduction

Rolling and sliding are the two major local deformation mechanisms between contacting particles in granular materials. These mechanisms control the overall behavior of granular materials. Whereas sliding tends to dissipate energy through friction, rolling is a deformation mode available to the granular material to mitigate energy dissipation. In classical microscopic theories of strength and dilatancy of granular media, sliding is considered to be the dominant factor controlling the microscopic deformation of granular materials. For example, the shear strength and dilatancy of soils have been explained by pure sliding (Horne, 1965, 1969; Newland & Allely, 1957; Rowe, 1962; Shodja & Nezami, 2003) while neglecting effects from particle rolling. However, it has been recognized that particle rotation and rolling between particles play important roles in the mechanical behavior of granular materials, especially in those composed of circular or spherical particles. From experiments (Skinner, 1969), rolling is observed to become dominant as inter-particle friction increases. Oda, Konishi, and Nemat-Nasser (1982) also reported from their biaxial compression tests that inter-particle rolling dominates the micro-scale deformation of granular media.

If the discrete element method (DEM) is used to analyze the behavior of granular materials (Cundall & Strack, 1979), the overall effect of grain rotation on the strength of shear bands and the amount of energy dissipation in granular material can be studied. Bardet et al. (Bardet, 1994; Bardet & Proubet, 1991) examined the structure of shear bands in granular materials by numerically simulating idealized granular media. They showed that particle rotations concentrate inside shear bands and found that rotations have significant effects on shear strength of granular materials. Alonso-Marroquin, Vardoulakis, Hermann, Weatherley, and Mora (2006) and Mora and Place (1998) showed that the rolling mode between particles leads to a significant reduction of macroscopic frictional dissipation, supporting the idea that rolling provides a possible mechanism for the heat-flow paradox in the study of earthquake dynamics (Henyey & Wasserburg, 1971; Lachenbruch & Sass, 1992).

If spherical particles are adopted in the DEM, the calculated macroscopic friction is limited to very low values because of excessive rolling of the particles, and local friction has a limited effect on the macroscopic shear strength (Oda et al., 1982). This situation can be improved using non-spherical particles (Ng, 2009; Salot, Gotteland, & Villard, 2009), or by introducing more complex contact laws including an additional rolling resistance (Iwashita & Oda,

* Corresponding author. Tel.: +61 49232576.
E-mail addresses: yucang_wang@hotmail.com, y.wang2@cqu.edu.au (Y. Wang).

http://dx.doi.org/10.1016/j.partic.2015.01.006
1674-2001/

Nomenclature

$\mathbf{n}$	a unit vector pointing from the center of particle 1 to the center of particle 2
$\mathbf{r}_1, \mathbf{r}_2$	position vectors of particles 1 and 2
$\mathbf{r}_c$	position vector of the contact point between two particles
$\mathbf{r}_{p1}, \mathbf{r}_{p2}$	vectors from the particle center to the contact point
R_1, R_2	radii of particles 1 and 2
$\mathbf{v}_1, \mathbf{v}_2$	linear velocity vectors of particles 1 and 2
$\mathbf{v}_{1n}, \mathbf{v}_{2n}$	normal components of $\mathbf{v}_1$ and $\mathbf{v}_2$ along vector $\mathbf{n}$
$\mathbf{v}_{1t}, \mathbf{v}_{2t}$	tangential components of $\mathbf{v}_1$ and $\mathbf{v}_2$ perpendicular to vector $\mathbf{n}$
$\mathbf{v}_c$	contact velocity vector of the particle pair
$\mathbf{v}_{ct}$	tangential component of the contact velocity $\mathbf{v}_c$
$\mathbf{v}_1^c, \mathbf{v}_2^c$	material velocities of the contact point in two particles
$\mathbf{v}_{1t}^c, \mathbf{v}_{2t}^c$	tangential components of $\mathbf{v}_1^c$ and $\mathbf{v}_2^c$
$\mathbf{s}_1, \mathbf{s}_2$	objective velocities of particles 1 and 2
$\mathbf{s}_{1r}, \mathbf{s}_{2r}$	components of $\mathbf{s}_1$ and $\mathbf{s}_2$ that contribute to rolling velocity
$\mathbf{s}_{1s}, \mathbf{s}_{2s}$	components of $\mathbf{s}_1$ and $\mathbf{s}_2$ that contribute to sliding velocity
$\boldsymbol{\omega}_1, \boldsymbol{\omega}_2$	angular velocities of particles 1 and 2
$\boldsymbol{\omega}_{1n}, \boldsymbol{\omega}_{2n}$	normal components of $\boldsymbol{\omega}_1$ and $\boldsymbol{\omega}_2$ along vector $\mathbf{n}$
$\boldsymbol{\omega}_{1t}, \boldsymbol{\omega}_{2t}$	tangential components of $\boldsymbol{\omega}_1$ and $\boldsymbol{\omega}_2$ perpendicular to the vector $\mathbf{n}$
$\boldsymbol{\omega}_{rb}$	overall angular velocity of the common rotating reference frame with respect to the global system
$\boldsymbol{\omega}_{rbs}$	angular velocity of rigid-body spinning
$\boldsymbol{\omega}_{rbr}$	angular velocity of rigid-body rotation
$\boldsymbol{\omega}_{pt}$	angular velocity of pure twisting between two particles

Acronyms

RB	rigid-body motion: two particles move together as a single rigid body
RBT	rigid-body translation: the particle pair has a rigid-body translational motion
RBR	rigid-body rotation: two particles rotate together as a single rigid body
RBS	rigid-body spinning: two particles spin together as a single rigid body around the vector $\mathbf{n}$
PR	pure rolling: two particles rotate over each other in a gear-like fashion
PS	pure sliding: occurs when the only motion is both particles rotating with the same angular velocity
PT	pure twisting between two particles

1998; Plassiard, Belheine, & Donz, 2009). Rolling resistance models are widely used by DEM researchers. Iwashita and Oda (1998, 2000) noted that the conventional DEM could not reproduce the large voids and high rotational gradients observed in shear band experiments. They found that rolling resistance causes arching at the contacts, permitting the easy formation of voids in physical tests. Therefore they proposed a modified model of the conventional DEM that took rolling resistance into account. Tordesillas et al. (Tordesillas, Peters, & Muthuswamy, 2005; Tordesillas & Walsh, 2002) incorporated rolling resistance in the DEM and examined the influence of particle rotation and rolling resistance in the rigid flat-punch problem, and found that extensive particle rotations occur near the edges of punch where there are high stress concentrations. These rotations lead to dilatation in the region adjacent to the sides of the punch. Wang and Mora (2008) showed that when only normal forces are transmitted, or rolling resistance is absent, the laboratory tests of wing-crack extension cannot be reproduced.

Quantitative investigation of the effects of rolling and sliding using the DEM demands a clear and unambiguous definition and calculation of rolling and sliding deformation. In principle, the relative motion between two particles in contact can be decomposed into several independent components: relative motion in the normal direction, relative motion in the tangential direction, or sliding, relative rolling, and in the 3-D case, relative twisting. However, even for the simplest 2-D case involving circular particles, there is surprisingly no agreement on what is the best way to define rolling and sliding. Various versions of definitions and calculations of rolling and sliding were proposed (Ai, Chen, Rotter, & Ooi, 2011; Alonso-Marroquin et al., 2006; Bagi & Kuhn, 2004; Bardet, 1994; Bardet & Proubet, 1991; Iwashita & Oda, 1998; Jiang, Yu, & Harris, 2005; Kuhn & Bagi, 2004a, 2004b; Luding, 2008; Mohamed & Gutierrez, 2010; Tordesillas et al., 2005; Tordesillas & Walsh, 2002). Some sources directly contradict others, confusing researchers in the DEM field. This even leads some researchers to suggest that there is no unique way to define rolling displacement (Bagi & Kuhn, 2004).

Based on clear definitions of pure rolling and sliding, Wang, Alonso-Marroquin, Xue, and Xie (2015) derived the rolling and sliding components in a simple way. They found that a conceptual mistake had been made in some previous models when dealing with pure sliding. After correcting the mistake, Iwashita–Oda's derivation and subsequently others produced correct results. Hence, they argued that there is indeed a unique way to determine the rolling velocity in the 2-D case. Rolling and sliding in the general 3-D case are more complicated. Currently there are only a few 3-D rolling models discussed in the literature (Bagi & Kuhn, 2004; Kuhn & Bagi, 2004a, 2004b; Luding, 2008), which do not agree with each other. The motivation of this paper is to derive rolling and sliding velocities in the 3-D case and to resolve the inconsistencies in rolling velocities found in the literature. As the method used to derive the 2-D rolling velocity is not general and cannot be applied to the 3-D case directly, in this paper we study the 3-D rolling problem by adopting a general vectorial notation developed in the previous papers (Alonso-Marroquin et al., 2006; Bagi & Kuhn, 2004; Kuhn & Bagi, 2004a, 2004b; Luding, 2008). This method is strict, unique, and objective.

Problem statement

Fig. 1 shows the kinematics of two particles indexed by 1 and 2. During a time step from t to $t+\Delta t$, two particles 1 and 2, with radii R_1 and R_2, respectively, remain in contact. Let $\mathbf{r}_1$ and $\mathbf{r}_2$ be the position vectors of the two particles, $\mathbf{v}_1$ and $\mathbf{v}_2$ be their linear velocity vectors, $\boldsymbol{\omega}_1$ and $\boldsymbol{\omega}_2$ be their angular velocities. Now the question is: for any arbitrary 3-D case, is there a unique way to determine rolling and sliding components? If the answer is yes, how? To answer these questions, we first need to define rigid-body (RB) velocity, objective velocities, pure rolling, and sliding.

Definition

Rigid-body velocity and objective velocities

A general vectorial notation developed in previous papers (Alonso-Marroquin et al., 2006; Bagi & Kuhn, 2004; Kuhn & Bagi, 2004a, 2004b; Luding, 2008) is followed here. Let $\mathbf{n}$ be a unit vector pointing from the center of particle 1 to the center of particle 2:

$$\mathbf{n} = \frac{\mathbf{r}_2 - \mathbf{r}_1}{|\mathbf{r}_2 - \mathbf{r}_1|} \approx \frac{\mathbf{r}_2 - \mathbf{r}_1}{R_1 + R_2}, \tag{1}$$

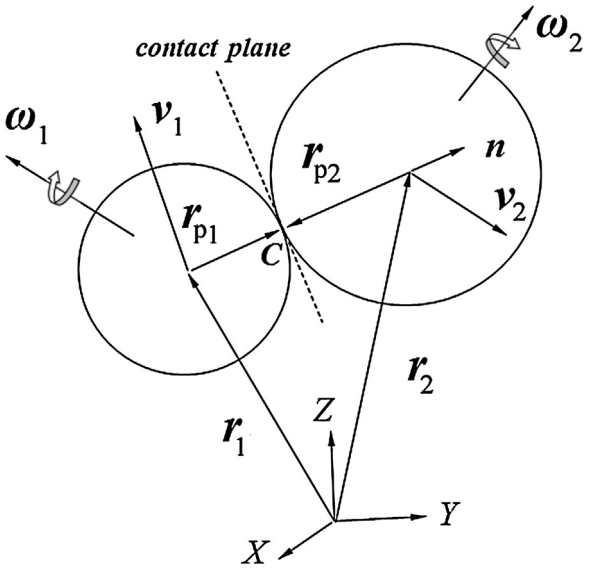

Fig. 1. Kinematics of two spherical particles in momentary contact.

where the approximation is valid only when the normal deformation is much smaller than the diameter of the particles (we assume this is true throughout this paper). For particle i ($i = 1, 2$), the velocity can be decomposed into two parts: the component along $\mathbf{n}$ and the component perpendicular to $\mathbf{n}$, which is on the contact plane:

$$\mathbf{v}_i = \mathbf{v}_{in} + \mathbf{v}_{it}, \quad i = 1, 2 \tag{2}$$

where the normal components are

$$\mathbf{v}_{in} = (\mathbf{v}_i \cdot \mathbf{n})\mathbf{n}, \quad i = 1, 2 \tag{3}$$

and the tangential components are

$$\mathbf{v}_{it} = \mathbf{v}_i - (\mathbf{v}_i \cdot \mathbf{n})\mathbf{n}, \quad i = 1, 2 \tag{4}$$

Let us define the branch vector as the vector connecting the centers of mass of the two particles. The position of the point attached to the branch vector at the contact is

$$\mathbf{r}_c = \mathbf{r}_1 + \mathbf{r}_{p1} = \mathbf{r}_1 + R_1\mathbf{n}. \tag{5}$$

The *contact velocity* is defined as the velocity of this point,

$$\mathbf{v}_c = \frac{d\mathbf{r}_c}{dt} = \mathbf{v}_1 + \frac{R_1}{R_1 + R_2}(\mathbf{v}_2 - \mathbf{v}_1) = \frac{R_1\mathbf{v}_2 + R_2\mathbf{v}_1}{R_1 + R_2}. \tag{6}$$

As we are only interested in the rolling and sliding motions between the two particles, which occur on the contact plane, we define the *rigid-body* (RB) *velocity* as the tangential component of the contact velocity,

$$\mathbf{v}_{ct} = \mathbf{v}_c - (\mathbf{v}_c \cdot \mathbf{n})\mathbf{n} = \frac{R_1\mathbf{v}_{2t} + R_2\mathbf{v}_{1t}}{R_1 + R_2}. \tag{7}$$

Let us consider two points attached to each particle, in a region infinitely near to the contact point. The material velocity of the point of contact has two possible values depending on which particle it is assumed to belong to. The velocities of these points can be determined in terms of the linear and angular velocities of the two particles:

$$\mathbf{v}_1^c = \mathbf{v}_1 + \boldsymbol{\omega}_1 \times \mathbf{r}_{p1}, \tag{8}$$

$$\mathbf{v}_2^c = \mathbf{v}_2 + \boldsymbol{\omega}_2 \times \mathbf{r}_{p2}. \tag{9}$$

Their tangential components are given as:

$$\mathbf{v}_{1t}^c = \mathbf{v}_{1t} + \boldsymbol{\omega}_1 \times \mathbf{r}_{p1}, \tag{10}$$

$$\mathbf{v}_{2t}^c = \mathbf{v}_{2t} + \boldsymbol{\omega}_2 \times \mathbf{r}_{p2}. \tag{11}$$

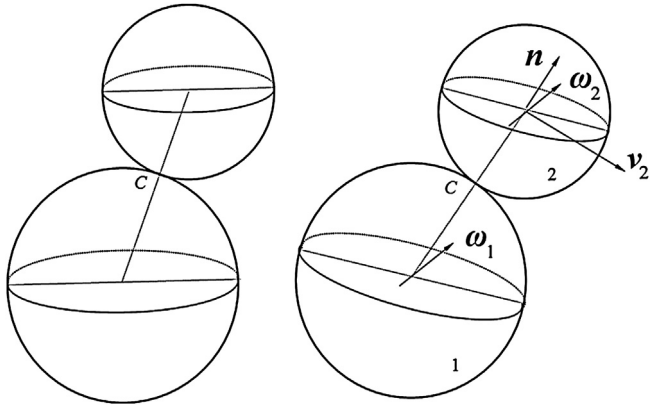

Fig. 2. Rigid-body rotation (RBR): two particles rotate together as a single rigid body. The left figure is the initial state. In this plot the velocity of the first particle is zero ($\mathbf{v}_1 = 0$), or the two particles rotate around the center of particle 1. The equator of each sphere represents its orientation.

The *objective velocities* of the two particles at the contact can be defined as the velocities of material points of Eqs. (10) and (11) subtracted by the RB velocity:

$$\mathbf{s}_1 = \mathbf{v}_{1t}^c - \mathbf{v}_{ct} = \boldsymbol{\omega}_1 \times \mathbf{r}_{p1} - \frac{R_1(\mathbf{v}_{2t} - \mathbf{v}_{1t})}{R_1 + R_2},$$

$$\mathbf{s}_2 = \mathbf{v}_{2t}^c - \mathbf{v}_{ct} = \boldsymbol{\omega}_2 \times \mathbf{r}_{p2} + \frac{R_2(\mathbf{v}_{2t} - \mathbf{v}_{1t})}{R_1 + R_2}.$$

Considering $\mathbf{r}_{p1} = R_1\mathbf{n}$ and $\mathbf{r}_{p2} = -R_2\mathbf{n}$, we have

$$\mathbf{s}_1 = R_1\boldsymbol{\omega}_1 \times \mathbf{n} - \frac{R_1(\mathbf{v}_{2t} - \mathbf{v}_{1t})}{R_1 + R_2}, \tag{12}$$

$$\mathbf{s}_2 = -R_2\boldsymbol{\omega}_2 \times \mathbf{n} + \frac{R_2(\mathbf{v}_{2t} - \mathbf{v}_{1t})}{R_1 + R_2}. \tag{13}$$

These two velocities are objective in the sense that their magnitudes are not affected by the common RB motion of the particle pair, to be shown below.

RB motion occurs when two particles move together as a single rigid body. In this case, the distance between any arbitrary chosen points on the two particles remains constant during the motion. There are three special RB cases. The first case is the rigid-body translation (RBT): the particle pair has a RB translational motion, and both particles have no rotation ($\mathbf{n}$ is a constant vector). RBT can be mathematically expressed as:

$$\mathbf{v}_1 = \mathbf{v}_2 \neq 0, \tag{14a}$$

$$\boldsymbol{\omega}_1 = \boldsymbol{\omega}_2 = 0. \tag{14b}$$

The second special RB case is the rigid-body rotation (RBR): two particles rotate together as a single RB (as a special case of RBR, $\mathbf{n}$ is rotating around the center of particle 1, as shown in Fig. 2). RBR can be mathematically expressed as:

$$\boldsymbol{\omega}_1 = \boldsymbol{\omega}_2 \neq 0, \tag{15a}$$

$$\boldsymbol{\omega}_1 \times \mathbf{n} \neq 0, \tag{15b}$$

$$\mathbf{v}_2 - \mathbf{v}_1 = \mathbf{v}_{2t} - \mathbf{v}_{1t} = (R_1 + R_2)\boldsymbol{\omega}_1 \times \mathbf{n}. \tag{15c}$$

Eq. (15c) is equivalent to

$$\boldsymbol{\omega}_1 = \boldsymbol{\omega}_2 = \boldsymbol{\omega}_{rbr} = \frac{\mathbf{n} \times (\mathbf{v}_2 - \mathbf{v}_1)}{R_1 + R_2}, \tag{15d}$$

where $\boldsymbol{\omega}_{rbr}$ is the angular velocity of the RBR.

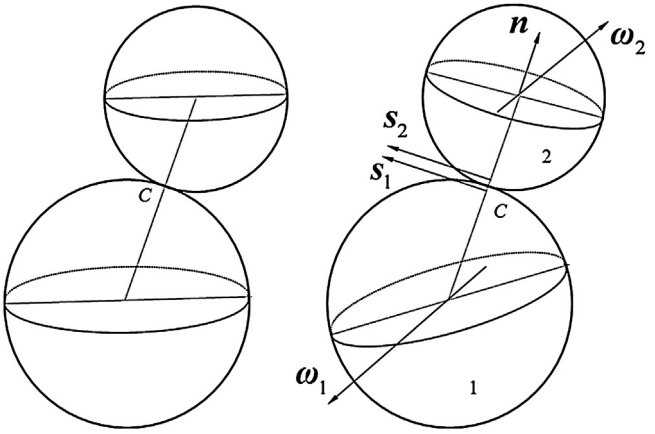

Fig. 3. Pure rolling (PR): two particles rotate over each other in a gear-like fashion. The left figure is the initial state.

The last special RB case is the rigid-body spinning (RBS): two particles spin together as a single RB around the vector **n**. RBS can be mathematically expressed as:

$$\boldsymbol{\omega}_1 = \boldsymbol{\omega}_2 \neq 0, \tag{16a}$$

$$\boldsymbol{\omega}_1 \times \mathbf{n} = 0, \tag{16b}$$

$$\mathbf{v}_1 = \mathbf{v}_2 = 0. \tag{16c}$$

From Eqs. (12) and (13), we obtain the following relation for all three special RB cases:

$$\mathbf{s}_1 = \mathbf{s}_2 = 0. \tag{17}$$

An arbitrary RB motion involves combinations of RBT, RBR, and RBS; therefore, $\mathbf{s}_1 = \mathbf{s}_2 = 0$ always holds for RB. This means that the objective velocities vanish if and only if the two particles move as a single RB.

If the two particles do not move as a single rigid body, the objective velocities involve rolling, sliding or accumulation of shear strain at the contact. To decompose the objective velocities into rolling and sliding velocity, we first need to define clearly and rigorously pure rolling and pure sliding.

Pure rolling and sliding

Pure rolling (PR)

PR occurs when two particles are rotating anti-parallel with angular velocities perpendicular to the normal direction **n**. In this case, the contact point is changing and no relative transverse displacement (or velocity) occurs at the contact point (Fig. 3). This can be mathematically expressed as:

$$\mathbf{v}_1 = 0, \quad \mathbf{v}_2 = 0; \tag{18a}$$

$$\boldsymbol{\omega}_1 \perp \mathbf{n}, \quad \boldsymbol{\omega}_2 \perp \mathbf{n}; \tag{18b}$$

$$\boldsymbol{\omega}_1 \times \mathbf{r}_{p1} = \boldsymbol{\omega}_2 \times \mathbf{r}_{p2}. \tag{18c}$$

The following two equations are found to hold for PR:

$$\mathbf{s}_2 = \mathbf{s}_1, \tag{19}$$

$$\boldsymbol{\omega}_2 = -\frac{R_1}{R_2}\boldsymbol{\omega}_1. \tag{20}$$

If $\boldsymbol{\omega}_1$ and $\boldsymbol{\omega}_2$ are constant vectors, the trajectories of the contact points in both particles are great circles perpendicular to $\boldsymbol{\omega}_1$ or $\boldsymbol{\omega}_2$.

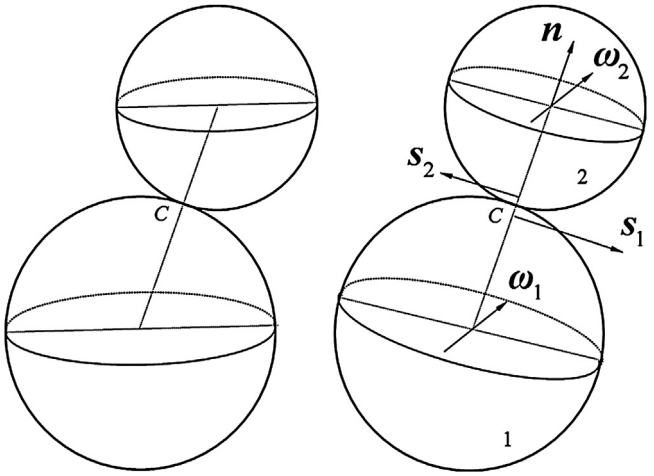

Fig. 4. Pure sliding (PS): two particles rotate with the same angular velocity. The left figure is the initial state.

Pure sliding (PS)

PS occurs when the only motion is both particles rotating with the same angular velocity perpendicular to the vector **n** (Fig. 4).

$$\mathbf{v}_1 = 0, \quad \mathbf{v}_2 = 0; \tag{21a}$$

$$\boldsymbol{\omega}_1 \perp \mathbf{n}, \quad \boldsymbol{\omega}_2 \perp \mathbf{n}; \tag{21b}$$

$$\boldsymbol{\omega}_1 = \boldsymbol{\omega}_2. \tag{21c}$$

As was pointed out by Wang et al. (2015), for PS,

$$\mathbf{s}_1 = -\mathbf{s}_2. \tag{22}$$

is only valid when $R_1 = R_2$, but not when $R_1 \neq R_2$. Instead, we use the following formula

$$\frac{\mathbf{s}_1}{R_1} = -\frac{\mathbf{s}_2}{R_2}. \tag{23}$$

Eq. (23) always holds for PS regardless of particle sizes. As will be pointed out in section "Comparison with earlier rolling models", Eq. (22) leads to incorrect calculations for rolling velocity.

From the definitions, it is clear that relative transverse velocity occurs, but there is no relative rotation between the two particles for PS, whereas for PR there must be relative rotation, but no relative transverse velocity between them. Therefore, PS does not have a PR component and vice versa. In other words, PS and PR are mutually independent.

Derivation of rolling and sliding in the general 3-D case

Generally, $\mathbf{v}_1, \mathbf{v}_2, \boldsymbol{\omega}_1$, and $\boldsymbol{\omega}_2$ can have arbitrary magnitudes and directions. However, the objective velocities of the two particles $\mathbf{s}_1$ and $\mathbf{s}_2$ are always on the contact plane, even though their magnitudes and directions can be arbitrary. From the linear independence of PR and PS, we can decompose both $\mathbf{s}_1$ and $\mathbf{s}_2$ into their PR and PS components (Fig. 5):

$$\mathbf{s}_1 = \mathbf{s}_{1r} + \mathbf{s}_{1s}, \tag{24}$$

$$\mathbf{s}_2 = \mathbf{s}_{2r} + \mathbf{s}_{2s}, \tag{25}$$

where $\mathbf{s}_{1s}$ and $\mathbf{s}_{2s}$ are the objective velocity components from the two particles contributing to PS, and $\mathbf{s}_{1r}$ and $\mathbf{s}_{2r}$ are the objective velocity components contributing to PR.

Considering Eq. (19) in PR and Eq. (23) in PS, we have the following two equations:

$$\mathbf{s}_{1r} = \mathbf{s}_{2r}, \quad \text{for PR}; \tag{26}$$

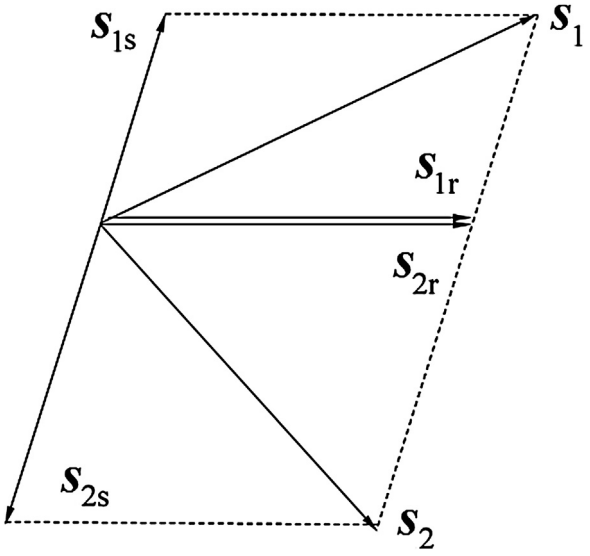

Fig. 5. The object velocities of the two particles $\mathbf{s}_1$ and $\mathbf{s}_2$ and their decomposition on the contact plane. $\mathbf{s}_{1s}$ and $\mathbf{s}_{2s}$ are components contributing to PS; $\mathbf{s}_{1r}$ and $\mathbf{s}_{2r}$ are components contributing to PR.

$$\frac{\mathbf{s}_{1s}}{R_1} = -\frac{\mathbf{s}_{2s}}{R_2}, \quad \text{for PS.} \tag{27}$$

Eqs. (24)–(27) have four unknown vectors, $\mathbf{s}_{1r}$, $\mathbf{s}_{1s}$, $\mathbf{s}_{2r}$, and $\mathbf{s}_{2s}$; hence unique solutions exist:

$$\mathbf{s}_{1r} = \mathbf{s}_{2r} = \frac{R_2}{R_1+R_2}\mathbf{s}_1 + \frac{R_1}{R_1+R_2}\mathbf{s}_2, \tag{28}$$

$$\mathbf{s}_{1s} = -\frac{R_1}{R_1+R_2}(\mathbf{s}_2 - \mathbf{s}_1), \tag{29}$$

$$\mathbf{s}_{2s} = \frac{R_2}{R_1+R_2}(\mathbf{s}_2 - \mathbf{s}_1). \tag{30}$$

The rolling velocity component is $\mathbf{v}_r = \mathbf{s}_{1r} = \mathbf{s}_{2r}$, and therefore from Eqs. (12), (13), and (28) we have

$$\mathbf{v}_r = \frac{R_1R_2}{R_1+R_2}(\boldsymbol{\omega}_1 \times \mathbf{n} - \boldsymbol{\omega}_2 \times \mathbf{n}). \tag{31}$$

From Eqs. (12), (13), (29), and (30), the sliding velocity component can be calculated:

$$\mathbf{v}_s = \mathbf{s}_{2s} - \mathbf{s}_{1s} = -R_2\boldsymbol{\omega}_2 \times \mathbf{n} - R_1\boldsymbol{\omega}_1 \times \mathbf{n} + \mathbf{v}_{2t} - \mathbf{v}_{1t}. \tag{32}$$

Eqs. (31) and (32) give the rolling and sliding velocity for the general 3-D case. It can be seen from Eq. (31) that the rolling velocity depends only on the angular velocities of the two particles. In Eq. (32), the first and second terms are the contribution of particle rotations to sliding velocity, whereas the third and fourth terms are from the relative translational motion between the two particles. Eqs. (31) and (32) are *objective*, because any common rotation (rigid-body rotation) of the two particles vanishes in the derivation (Eqs. (17) and (28)–(30)). It can be seen that for PS, $\mathbf{v}_r = 0$ (see Eqs. (21a), (21c), and (31)), and for PR, $\mathbf{v}_s = 0$ (see Eqs. (18a), (20), and (32)). This further shows that PS and PR are independent.

Complete decomposition and special cases

Complete decomposition of the relative motion between two particles

It is evident from Eqs. (31) and (32) that the tangential components of particle velocities $\mathbf{v}_{it}$ do not contribute to the rolling velocity, but only contribute to the sliding velocity. The normal components of the particle velocities $\mathbf{v}_{in}$ have no influence on either the rolling velocity or the sliding velocity. Instead, they contribute to the normal relative velocity by

$$\mathbf{v}_n = \mathbf{v}_{2n} - \mathbf{v}_{1n} = ((\mathbf{v}_2 - \mathbf{v}_1)\cdot\mathbf{n})\mathbf{n}. \tag{33}$$

Similar to Eqs. (2)–(4), the angular velocity can also be decomposed into two parts:

$$\boldsymbol{\omega}_i = \boldsymbol{\omega}_{in} + \boldsymbol{\omega}_{it}, \quad i = 1, 2 \tag{34}$$

where the normal components are

$$\boldsymbol{\omega}_{in} = (\boldsymbol{\omega}_i \cdot \mathbf{n})\mathrm{n}, \quad i = 1, 2 \tag{35}$$

and the tangential components are

$$\boldsymbol{\omega}_{it} = \boldsymbol{\omega}_i - (\boldsymbol{\omega}_i \cdot \boldsymbol{n})\mathbf{n}, \quad i = 1, 2 \tag{36}$$

Because $\boldsymbol{\omega}_i \times \mathbf{n} = \boldsymbol{\omega}_{it} \times \mathbf{n}$ ($i = 1, 2$), the contributions of angular velocities to the rolling and the sliding velocity (Eqs. (31) and (32)) are actually from $\boldsymbol{\omega}_{it}$. The contribution of $\boldsymbol{\omega}_{in}$ is discussed below.

If $\boldsymbol{\omega}_{1n} = \boldsymbol{\omega}_{2n}$, the particle pair spin as a single rigid-body (RBS); if $\boldsymbol{\omega}_{1n} = -\boldsymbol{\omega}_{2n}$, pure twisting (PT) occurs. For the general case, the motion induced by $\boldsymbol{\omega}_{in}$ can be decomposed into two independent parts corresponding to RBS and PT:

$$\boldsymbol{\omega}_{rbs} = \frac{1}{2}(\boldsymbol{\omega}_{1n} + \boldsymbol{\omega}_{2n}), \tag{37}$$

$$\boldsymbol{\omega}_{pt} = \frac{1}{2}(\boldsymbol{\omega}_{2n} - \boldsymbol{\omega}_{1n}). \tag{38}$$

Therefore, any arbitrary relative motion between the two particles can be decomposed into four independent parts: the normal relative motion (Eq. (33)), sliding (PS, Eq. (32)), rolling (PR, Eq. (31)) and twisting (PT, Eq. (38)).

We can define the *common rotating reference frame* as the coordinate system with its z-axis oriented parallel to $\mathbf{n}$ and the x- and y-axes rotating around $\mathbf{n}$ with angular velocity $\boldsymbol{\omega}_{rbs}$. As $\mathbf{n}$ may rotate with respect to the global system (Eq. (15d)), the overall angular velocity of the common rotating reference frame with respect to the global system is

$$\boldsymbol{\omega}_{rb} = \boldsymbol{\omega}_{rbs} + \boldsymbol{\omega}_{rbr} = \frac{1}{2}(\boldsymbol{\omega}_{1n} + \boldsymbol{\omega}_{2n}) + \frac{\mathbf{n} \times (\mathbf{v}_2 - \mathbf{v}_1)}{R_1 + R_2}. \tag{39}$$

The RB motion (RBT, RBR and RBS) has no influence on the four basic kinds of relative motion described by Eqs. (31)–(33), and (38), and vanishes in the common rotating reference frame.

Special cases

Two special cases are discussed here. In the 2-D case, $\mathbf{v}_1$ and $\mathbf{v}_2$ are limited in the $x-y$ plane, $\boldsymbol{\omega}_1$ and $\boldsymbol{\omega}_2$ in the $\pm z$ direction. The six vectors in Fig. 5 ($\mathbf{s}_1$, $\mathbf{s}_2$, $\mathbf{s}_{1r}$, $\mathbf{s}_{1s}$, $\mathbf{s}_{2r}$, and $\mathbf{s}_{2s}$) align in the same straight line. If we assume that counter-clockwise angular velocities are positive, and $\mathbf{t} = \mathbf{n} \times \mathbf{k}$ is the unit tangent vector at the contact point C, with $\mathbf{k}$ a unit vector in the z-direction, then Eqs. (31) and (32) become scalar quantities:

$$v_r = \frac{R_1R_2}{R_1+R_2}(\omega_1 - \omega_2), \tag{40}$$

$$v_s = R_1\omega_1 + R_2\omega_2 + v_{2t} - v_{1t}. \tag{41}$$

These are exactly the rolling and sliding velocities derived by Wang et al. (2015). This means that the general 2-D situation is a special case of the 3-D analysis.

The second case is a special case of rolling: two particles rotate like bevel gears (Fig. 6). In this case, the vectors $\boldsymbol{\omega}_1$ and $\boldsymbol{\omega}_2$ are not anti-parallel, but stay in the same plane and remain constant with respect to the global frame. As Eqs. (18a) and (18c) both hold but Eq. (18b) does not, there is no relative transverse velocity at the contact point, indicating that this is rolling without a sliding component.

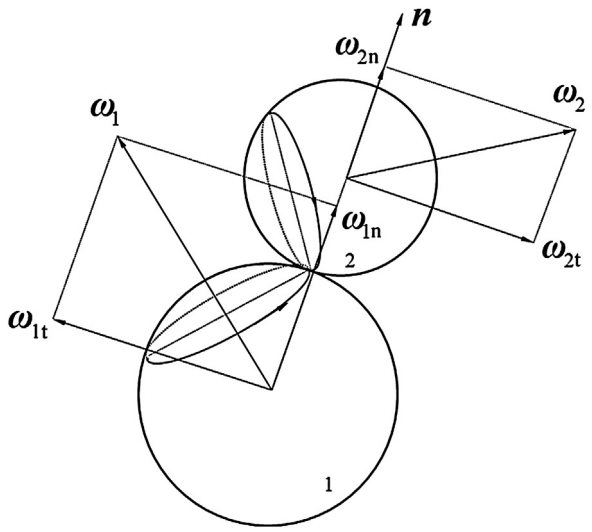

Fig. 6. A special case of rolling (but not pure rolling). Two particles rotate like bevel gears.

If we further assume that $\boldsymbol{\omega}_{1n} = \boldsymbol{\omega}_{2n}$, then twisting is not active. Observing from the common rotating reference frame, we would conclude that the two particles have pure rolling motion over each other at any instant moment, but $\boldsymbol{\omega}_{1t}$ and $\boldsymbol{\omega}_{2t}$ are always changing their directions, rotating round the normal direction $\mathbf{n}$ with angular velocity of $-\boldsymbol{\omega}_{1n}$. The trajectories of the contact points in both particles are small circles perpendicular to $\boldsymbol{\omega}_1$ and $\boldsymbol{\omega}_2$ (Fig. 6). From this example, we see that rolling directions in 3-D can change at any moment, which is not the case in the 2-D case.

The rolling and sliding velocities described by Eqs. (31) and (32) are valid for all special cases, which can similarly be analyzed and checked but is not repeated here.

Comparison with earlier rolling models

Kuhn and Bagi (2004a, 2004b) and Bagi and Kuhn (2004) derived the following 2-D and 3-D rolling velocities (termed as "Type 2 rolling" or "the Iwashita-Oda rolling"):

$$v_r = \frac{1}{2}\left[R_1\omega_1 - R_2\omega_2 + \frac{R_2 - R_1}{R_1 + R_2}(\mathbf{v}_2 - \mathbf{v}_1)\cdot\mathbf{t}\right], \quad \text{for 2-D;} \tag{42}$$

$$\mathbf{v}_r = \frac{1}{2}\left[R_1\boldsymbol{\omega}_1 \times \mathbf{n} - R_2\boldsymbol{\omega}_2 \times \mathbf{n} + \frac{R_2 - R_1}{R_1 + R_2}(\mathbf{v}_{2t} - \mathbf{v}_{1t})\right], \quad \text{for 3-D;} \tag{43}$$

where $\mathbf{t}$ in Eq. (42) is the unit tangent vector at the contact point C.

Contrary to Eq. (31), Eqs. (42) and (43) imply that the linear velocities of the particles contribute directly to the rolling velocity when $R_2 \neq R_1$. If $R_2 = R_1$, the third terms in Eqs. (42) and (43) drop out, and Eq. (43) agrees with Eq. (31). However, a difficulty emerges in Eq. (43) in cases with different particle sizes. For example, for PS + RBR (Fig. 7), the particles do not rotate, and a zero rolling velocity should be expected. However, Eqs. (42) and (43) predict a non-zero rolling velocity coming from the third term. A more detailed discussion on the problems of Eq. (42) can be found in our recent paper (Wang et al., 2015).

The reason why Eqs. (42) and (43) were obtained is explained here. Iwashita and Oda (1998) wrote: "if *da* equals *db* pure sliding occurred without any particle rotation"; here *da* and *db* were the arcs corresponding to $\mathbf{s}_1\Delta t$ and $\mathbf{s}_2\Delta t$ in the paper. This statement is similar to Eq. (22), indicating that the following formula,

$$\mathbf{s}_{1s} = -\mathbf{s}_{2s}, \tag{44}$$

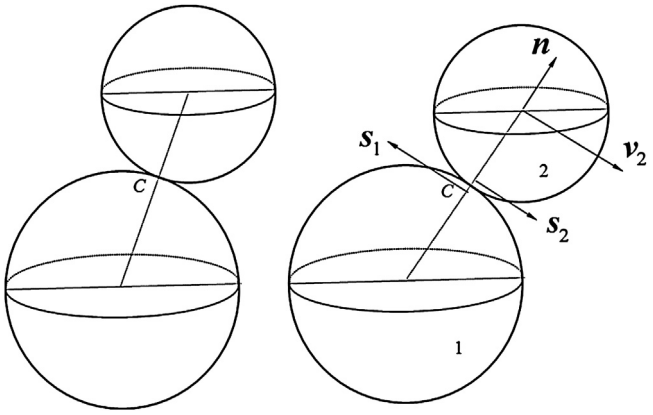

Fig. 7. Two particles do not rotate, but have a relative tangential displacement. The left figure is the initial state. This is PS + RBR if observed in the global frame, and PS if observed in the common rotating reference frame.

will replace Eq. (27). Solving Eqs. (24)–(26) and (44) yields the following solutions, instead of Eqs. (28)–(30):

$$\mathbf{s}_{1r} = \mathbf{s}_{2r} = \frac{1}{2}(\mathbf{s}_2 + \mathbf{s}_1), \tag{45}$$

$$\mathbf{s}_{1s} = -\frac{1}{2}(\mathbf{s}_2 - \mathbf{s}_1), \tag{46}$$

$$\mathbf{s}_{2s} = \frac{1}{2}(\mathbf{s}_2 - \mathbf{s}_1). \tag{47}$$

Eq. (45) implies that the rolling velocity is the arithmetic average of the movements of two material points, contrary to Eq. (28) where the rolling velocity is the weighted average. Consequently, the wrong rolling velocity of Eq. (43) was obtained based on Eqs. (12), (13), and (45). Note that the same sliding velocity of Eq. (32) is obtained using $\mathbf{v}_s = \mathbf{s}_{2s} - \mathbf{s}_{1s}$, even though $\mathbf{s}_{1s}$ and $\mathbf{s}_{2s}$ (Eqs. (46) and (47)) are not correct. It seems that Kuhn and Bagi (2004a, 2004b) and Bagi and Kuhn (2004) derived Eqs. (42) and (43) by directly defining the rolling velocity as Eq. (45), rather than following Iwashita and Oda's statement on PS (Eq. (44)). Our analysis shows that Eq. (45) is the direct consequence of Eq. (44). As discussed in Eqs. (22) and (23), Eq. (44) is not physically accurate, and is responsible for the failure of Eqs. (42) and (43) if $R_2 \neq R_1$, because this equation ignores the important physical picture that for PS, $da = db$ is only valid for $R_1 = R_2$, and does not hold when $R_1 \neq R_2$. Therefore, it is fair to say that Eq. (43) is correct only if $R_2 = R_1$. Meanwhile, we argue that the direct definition of rolling velocity in a general case is very difficult and prone to errors, as for Eq. (45). However, one exception is the correct rolling velocity directly defined by Luding (2008). Although no further explanation can be found in the literature, his formula is based on the principle of objectivity, and is identical to Eq. (31).

Concluding remarks

Rolling and sliding in 3-D are more complicated than in 2-D because they can always change direction. In this paper, we derived rolling and sliding velocities for the general 3-D case. First we calculated the material velocities of the contact points. These velocities, termed the objective velocities, vanish if the two particles move as a single rigid body. Then we defined pure rolling and pure sliding deformation between two particles. By these definitions, the correct rolling and sliding velocities in 3-D are derived.

The results show that any arbitrary relative motion between the two particles can be decomposed into four independent terms: normal relative motion, sliding, rolling and twisting. The derivations and results are objective, indicating that any common motion of the

two particles (moving as a single rigid-body) vanishes. The rolling and sliding velocities derived in this paper reduced to the 2-D case, and the results were valid in all special cases tested.

As a core result, we pointed out that the Iwashita–Oda rolling model fails to predict the correct rolling velocity when two particles have different sizes. The failure was caused by either misunderstanding the properties in pure rolling or the direct definition of rolling velocity in the general case in a seemingly reasonable way, which was actually found to be physically incorrect. After correcting the mistakes, Iwashita–Oda's rolling velocity and those subsequent came to the correct result. Compared with the direct definition of rolling velocity in the general case in the previous studies, our derivations based on the definitions of pure rolling and sliding motion are simpler, more fundamental, and less prone to mistakes. We conclude that there is indeed a unique way to define rolling displacement in the 3-D case, and that rolling and sliding are completely decomposable.

Acknowledgments

YW wishes to express his gratitude to Huainan Coal Mining Group in China and CSIRO in Australia for their financial support of this study. FAM acknowledges the support of The University of Sydney Civil Engineering Research Development Scheme (CERDS) scheme, and discussions with Stefan Luding and Sean McNamara.

References

Ai, J., Chen, J. F., Rotter, J. M., & Ooi, J. Y. (2011). Assessment of rolling resistance models in discrete element simulations. *Powder Technology*, *206*, 269–282.

Alonso-Marroquin, F., Vardoulakis, I., Herrmann, H. J., Weatherley, D., & Mora, P. (2006). Effect of rolling on dissipation in fault gouges. *Physical Review E*, *74*, 031306.

Bagi, K., & Kuhn, M. R. (2004). A definition of particle rolling in a granular assembly in terms of particle translations and rotations. *Journal of Applied Mechanics*, *71*, 493–501.

Bardet, J. P. (1994). Observations on the effects of particle rotations on the failure of idealized granular materials. *Mechanics of Materials*, *18*, 159–182.

Bardet, J. P., & Proubet, J. (1991). A numerical investigation of the structure of persistent shear bands in granular media. *Geotechnique*, *41*, 599–613.

Cundall, P. A., & Strack, O. D. L. (1979). A discrete numerical model for granular assemblies. *Geotechnique*, *29*, 47–65.

Henyey, T. L., & Wasserburg, G. J. (1971). Heat flow near major strike-slip faults in central and southern California. *Journal of Geophysical Research*, *76*, 7924–7946.

Horne, M. R. (1965). The behaviour of an assembly of rotund, rigid, cohesionless particles. I and II. *Proceedings of the Royal Society A*, *286*(62–78), 79–97.

Horne, M. R. (1969). The behaviour of an assembly of rotund, rigid, cohesionless particles. III. *Proceedings of the Royal Society A*, *310*, 21–34.

Iwashita, K., & Oda, M. (1998). Rolling resistance at contacts in simulation of shear band development by DEM. *Journal of Engineering Mechanics*, *124*, 285–292.

Iwashita, K., & Oda, M. (2000). Micro-deformation mechanism of shear banding process based on modified distinct element method. *Powder Technology*, *109*, 192–205.

Jiang, M. J., Yu, H. S., & Harris, D. (2005). A novel discrete model for granular material incorporating rolling resistance. *Computers and Geotechnics*, *32*, 340–357.

Kuhn, M. R., & Bagi, K. (2004a). Alternative definition of particle rolling in a granular assembly. *Journal of Engineering Mechanics*, *130*, 826–835.

Kuhn, M. R., & Bagi, K. (2004b). Contact rolling and deformation in granular media. *International Journal of Solids and Structures*, *41*, 5793–5820.

Lachenbruch, A. H., & Sass, J. H. (1992). Heat flow from Cajon Pass, fault strength and tectonic implications. *Journal of Geophysical Research*, *97*, 4995–5015.

Luding, S. (2008). Cohesive, frictional powders: Contact models for tension. *Granular Matter*, *10*, 235–246.

Mohamed, A., & Gutierrez, M. (2010). Comprehensive study of the effects of rolling resistance on the stress–strain and strain localization behavior of granular materials. *Granular Matter*, *12*, 527–541.

Mora, P., & Place, D. (1998). Numerical simulation of earthquake faults with gouge: Towards a comprehensive explanation for the heat flow paradox. *Journal of Geophysical Research*, *103*, 21067–21089.

Newland, P. L., & Allely, B. H. (1957). Volume changes in drained taixial tests on granular materials. *Geotechnique*, *7*, 17–34.

Ng, T. T. (2009). Particle shape effect on macro- and micro-behaviors of monodisperse ellipsoids. *International Journal for Numerical and Analytical Methods in Geomechanics*, *33*, 511–527.

Oda, M., Konishi, J., & Nemat-Nasser, S. (1982). Experimental micromechanical evaluation of strength of granular materials: Effects of particle rolling. *Mechanics of Materials*, *1*, 269–283.

Plassiard, J. P., Belheine, N., & Donz, F. V. (2009). A spherical discrete element model: Calibration procedure and incremental response. *Granular Matter*, *11*, 293–306.

Rowe, P. W. (1962). The stress-dilatancy relation for static equilibrium of an assembly of particles in contact. *Proceedings of the Royal Society, London, Series A*, *269*, 500–527.

Salot, C., Gotteland, P., & Villard, P. (2009). Influence of relative density on granular materials behavior: DEM simulations of triaxial tests. *Granular Matter*, *11*, 221–223.

Shodja, H. M., & Nezami, E. G. (2003). A micromechanical study of rolling and sliding contacts in assemblies of oval granules. *International Journal for Numerical and Analytical Methods in Geomechanics*, *27*, 403–424.

Skinner, A. E. (1969). A note on the influence of interparticle friction on the shearing strength of a random assembly of spherical particles. *Geotechnique*, *19*, 150–157.

Tordesillas, A., & Walsh, D. C. S. (2002). Incorporating rolling resistance and contact anisotropy in micromechanical models of granular media. *Powder Technology*, *124*, 106–111.

Tordesillas, A., Peters, J., & Muthuswamy, M. (2005). Role of particle rotations and rolling resistance in a semi-infinite particulate solid indented by a rigid flat punch. *ANZIAM Journal*, *46*, 260–275.

Wang, Y. C., & Mora, P. (2008). Modeling wing crack extension: Implications for the ingredients of discrete element model. *Pure and Applied Geophysics*, *165*, 609–620.

Wang, Y. C., Alonso-Marroquin, F., Xue, S., & Xie, J. (2015). Revisiting rolling and sliding in two-dimensional discrete element models. *Particuology*, *18*, 35–41.